Characterisation Methods

Contact Angle

It is common experience that a liquid drop placed on a flat surface shows a tendency to configure its shape more or less flat according to the characteristics of the surface and liquid used. The more the liquid is alike to the solid surface, the more the drop will be flat. Instead, if between solid and liquid there are not appreciable interactions, the drop will have a shape more similar to a sphere, to minimise contact with the solid. To quantify of this phenomenon, the contact angle, defined as the angle (θ), that the horizontal solid surface makes with the tangent to liquid-air interface, drawn from the point of contact drop-solid surface (fig.1).

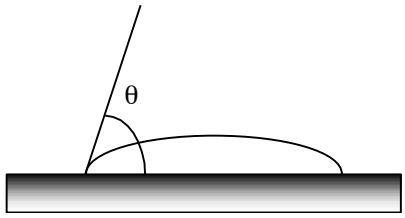

Fig.1 Schematic description of contact angle.

The measurement of contact angle measure gives an elegant and simple method to characterise the interfacial properties of a solid substrate and, moreover, allows the biological compatibility of surfaces to be studied [1].
The measurement is based on the following principles:

1. the solid surface is rigid, unmoveable, and non-deformable. In practise, it means that elastic modulus of surface must be greater than 3.5 N/cm^2;
2. the solid surface is almost smooth, so it is possible ignore the hysteris effects associated with the roughness of material;
3. the solid surface is uniform and homogenous;
4. the surface tension of the liquid is well known and constant and does not change during the experiment;
5. the solid surface does not interact with the liquid, even during the equilibrium between the three liquid-solid-aeroform phases;
6. the diffusion pressure of the liquid on the solid is zero. It means that the liquid vapours are not absorbed by the solid and so they do not alter it;
7. the solid surface is so rigid and unmoveable that the superficial groups cannot direct or equilibrate themselves after environmental changes.

The most common methods of measuring of contact-angles are [2]:

a) direct measurement of the angle with an optical microscope at the interface between three phases with a goniometer;
b) measure of the dimensions of the profile of a drop on the surface. Using equations of spherical trigonometry the angle can be calculated;
c) measurement of the diameter of a drop of known volume on the surface;
d) measurement of the height variation of a liquid of known superficial tension in a capillary or on a vertical plate,
e) the Dunoy technique;
f) the Wilhelmy- plate method.

The contact angle gives some information on the affinity between solid and liquid and air. The relationship between contact angle and interfacial tensing is:

$$\cos\theta = \frac{\gamma_{s/a} - \gamma_{s/l}}{\gamma_{l/a}}$$

$\gamma_{s/a}$= interfacial solid-air tension
$\gamma_{s/l}$= interfacial solid-liquid tension
$\gamma_{l/a}$= interfacial liquid-air tension
If the contact angle is small (the drop is very flat), $\cos\theta \Rightarrow 1$,and so $\gamma_s/a-\gamma_s/l = \gamma_l/a$.
For example, if the liquid is water (γ_l/a =72.8 dyne/cm), this wets the solid if the interfacial solid-liquid tension is sufficiently small such that the numerator value remains at a value close to γ_l/a.
Putting, for example, a water drop on a silica planar surface it is possible to observed small contact angle due to the affinity between the water molecules and the silica. Water, infact, form dipole-dipole interactions or sometimes hydrogen bonds with the hydroxyl group of the solid. Instead, putting a water drop on a surface that has non-polar groups toward the outside, the drop will have a spherical shape, due to the repulsion between water molecules and non-polar groups. The cohesive forces between water molecules, in this case, are bigger that adhesion forces between these and the solid surface [3, 4, 5].
In this research work the methods used to measure the contact angle were:

- direct drop method;
- Bubble-air method.

Direct drop method
A drop with a diameter inferior to a mm is placed on a surface (the small dimensions allow to minimise the deviations due to the weight of the liquid that tends to flatten the drop) and, using an optical microscope with the objective directed horizontally, it is possible to measure the value of θ or, more commonly, the height and the width of the drop. In this case using simple trigonometric relationship we can calculate the value of contact angle (fig.2).

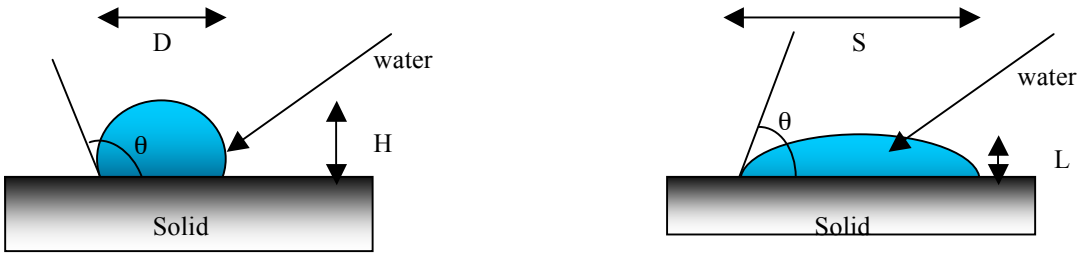

θ>90°
θ =180°-arcos (2H/D-1)

θ<90°
θ =2 arctan (2L/S)

Fig.2 Direct drop method.

"Bubble-air" method
The surface is dipped in the liquid, and with a needle with a "U" form, small airdrops adhere at inferior surface (also in this case the small dimension are important to minimise the effects of hydrostatic force). With a device similar to the above it is possible to measure the dimensions of air drops and hence calculate the contact angle (fig. 3).

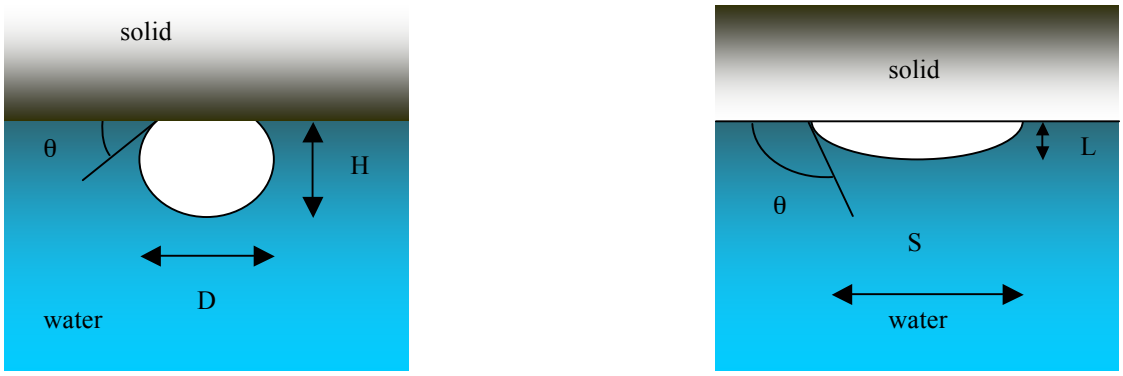

θ<90°
θ = arcos (2H/D –1)

θ>90°
θ = 180°- 2 arctan (2L/S)

Fig.3 "Bubble-air" method.

The error of these methods is due to the hysteresis, in other words to the increase or decrease of contact angle during the measurement.
The three principal causes of hysteresis are:

1) the contamination of liquid or of the surface;
2) the presence of high roughness of material, that traps small quantities of air, altering the contact surface;
3) the rigidity of surface for which the positioning of bubble on the surface is difficult.

For these reasons, the measurements are not highly reproducible and there are variations in measured contact angle at different points on a surface.

Ellipsometry

Ellipsometry is a highly sensitive optical technique, useful for the thickness and optical density of a thin film [6].
Ellipsometry is defined as the measurement of the Polarisation State of a wave vector. From the state of polarisation after reflection at an interface it is possible to obtain information on to the optical constants of the system that interacted with light ray modulating its polarisation.
The ellipsometric parameters measured are the complex ratio between the reflection coefficients relative to wave vectors polarised parallel and perpendicular to the plane of incidence. The electromagnetic theory of light allows the interpretation of the ellipsometric data obtained, giving equation that relate the complex amplitudes of reflections coefficients to the macroscopic properties that characterise the structure under examination.
Making measurements in different points of a surface, it is possible evaluate the uniformity of the layer. The lowest value of thickness that can be measured with this

technique is almost an order of amplitude inferior than that measured with interferometric techniques, about 1 Angstrom.
In the theory, a light ray propagating along the Z-axis of a Cartesian system can be described as:

$$\begin{aligned} E_x &= a_1 \cos(\tau + \delta 1) \\ E_y &= a_2 \cos(\tau + \delta_2) \end{aligned} \quad (3.1)$$

where: $\tau = \omega\left(t - \frac{z}{v}\right)$ and ω is the angular frequency and v is linear speed of light. The total amplitude is the sum of vectors a_1 e a_2, while $\delta=\delta_2-\delta_1$ is the difference of phase of two components of the field.
In a stationary plane, the electric field is an ellipse. To study the variations of electric field after reflection on a surface, it is useful to utilise Poincarrè's sphere, with which it is possible represent elliptically polarised light. To utilise this principle it is necessary make a transformation of co-ordinates with the Stokes's parameters, S, given by:

$S_0=a_1^2+a_2^2$ (3.2)
$S_1= a_1^2-a_2^2$ (3.3)
$S_2= a_1a_2 \cos \delta$ (3.4)
$S_2= a_1a_2 \sin \delta$ (3.5)

Where S_1, S_2 and S_3 are the axes of the new Cartesian system of reference. Every point of this sphere represents a well-defined state of light polarisation. Infact, the light that is incident on the plane is represented by point P and, after reflection, it is represented by V, as illustrated in the figure 4 [7].

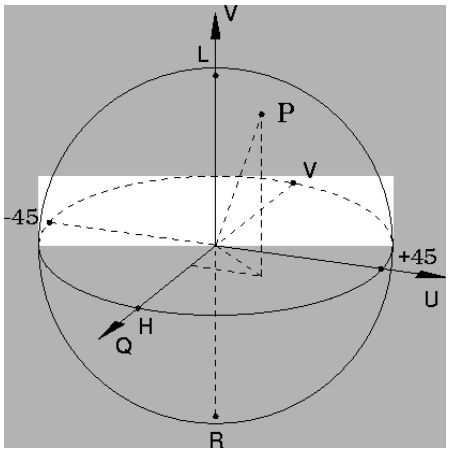

Fig.4 Poincarré's sphere.

The incident light can be separated into two components: one parallel and the other perpendicular to the plane of incidence. The reflection process introduces a phase difference Δ between these components and the variations in the ratio between their amplitudes, according to the law $\frac{|R_p|}{|R_s|}$ $tan\psi$, where $tan\psi$ represents a measure of the absorptions of the two components. For this reason, the ratio between the reflection coefficient of polarised light in the plane of incidence and that in the plane of the surface is given by:

$$\rho = \frac{r_p}{r_s} = \tan\psi \cdot e^{j\Delta} \quad (3.6)$$

where ρ is the ratio between the reflection coefficients, while ψ e Δ are functions of optical constants of surface, in other words of the wavelength of used light, the angle of incidence, thickness and refractive index of the film.

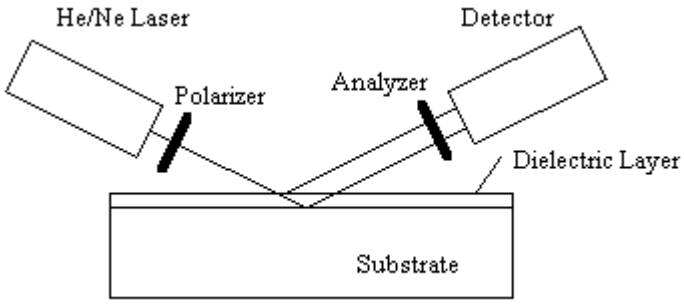

Fig.5 Scheme of an ellipsometer

A typical ellipsometer is schematised in figure 5. There is a compensator, which is of a birefractive plane with thickness of a quarter of a wavelength. This is used to convert the light linearly polarised in elliptically polarised light. The light polarised in this manner is incident on the sample and, after reflection, changes its characteristics. The polarisation of the reflected wave is measured with an analyser, and its intensity is recorded by a photoelectric detector. This technique has been used to measure the refractive index and the thickness of polymeric films spoon on coverslips. The system under examination is composed of a film of refractive index n_2 and thickness d on a reflective surface with index n_3, I a medium in a mean of index n_1 (as in figure 6). The medium is isotropic and non-absorbing, while the other refractive indices are complex. If we consider light incident at the boundary between the medium and the film, the cosine of the angle of refraction is given by:

$$\cos\phi_2 = \left[1 - \left(\frac{n_1}{n_2} sin\phi_1\right)^2\right]^{\frac{1}{2}} \quad (3.7)$$

while the parallel and normal coefficients for the incident light at boundary are given by:

$$r^p{}_{12} = \frac{n_2\cos\phi_1 - n_1\cos\phi_2}{n_2\cos\phi_1 + n_1\cos\phi_2}$$
$$r^n{}_{12} = \frac{n_1\cos\phi_1 - n_2\cos\phi_2}{n_1\cos\phi_1 + n_2\cos\phi_2} \quad (3.8)$$

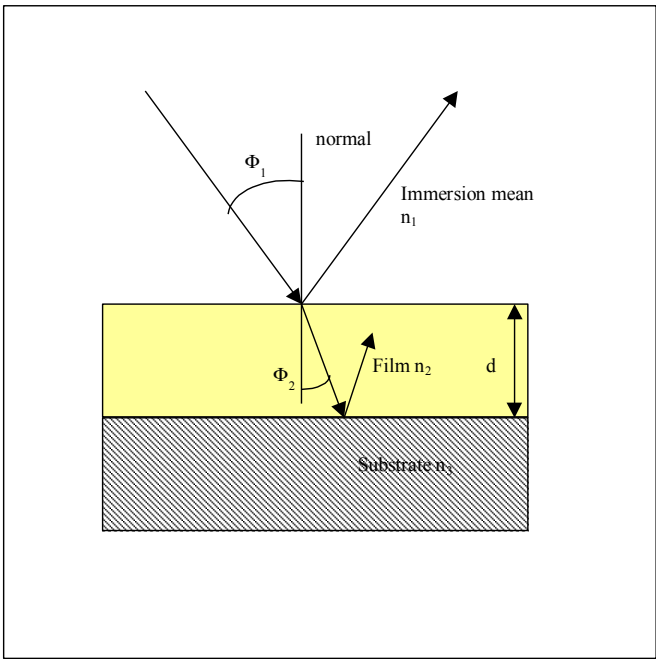

Fig.6 Reflection on a surface covered by a film.

The reflection coefficients at the boundary between the film and the substrate, r^p_{23} and r^n_{23} are given by similar expressions. The total reflection coefficients total R^p and R^n, that include the contribution of reflections of the lowest layers, are given by:

$$R^p = \frac{r^p{}_{12} + r^p{}_{23} \exp D}{1 + r^p{}_{12} r^p{}_{23} \exp D}$$

$$R^n = \frac{r^n{}_{12} + r^n{}_{23} \exp D}{1 + r^n{}_{12} r^n{}_{23} \exp D} \qquad (3.9)$$

where $\cos\phi_3$ is given by an expression similar to that of $\cos\phi_2$, while D is:

$$D = -4\pi \cdot jn_2 \cos\phi_2 \frac{d_2}{\lambda} \qquad (3.10)$$

λ is the wavelength of light.
The ratio between the parallel and normal reflection coefficient is defined by $\rho = R^p/R^n$, and can be also expressed as

$$\rho = \tan\psi \exp(j\Delta) \quad (3.11).$$

The values of ρ and Δ are determined by ellipsometric measurements and the refractive index of a surface can be determinated by following equation:

$$n_3 = n_1 \tan\phi_1 \left[1 - \frac{4\rho \cdot \sin^2\phi_1}{(\rho+1)^2}\right]^{\frac{1}{2}} \qquad (3.12)$$

where ϕ_1 is the angle of incidence.
To calculate the thickness of the film, equations (3.9), (3.10) and (3.12) can be combined to give the quadratic equation as:

$$C_1 (\exp D)^2 + C_2 (\exp D) + C_3 = 0 \quad (3.13)$$

Where the C coefficients are complex functions of the refractive index, angle of incidence and Δ and ψ. Once D is obtained by formula equation (3.10), it is possible to obtain the thickness *d,* choosing the value of thickness that only has a real part, or where the imaginary part is very small. For a thin layer system with a complex refractive index, the ellipsometry equation cannot be solved analytically, because the data input (Δ and ψ) are not sufficient to provide the output data (n_2, ε_2, d). Software based on error minimisation between experimental and predicted Δ,ψ values using the least squares method) was therefore developed in Matlab to estimate the thickness and the refractive index of polymer films.

Kelvin probe technique

It is well none that cells, owing to the nature of the cytoplasmic lipid membrane, present a small negative external electrical charge. Interaction with positive surface are thus favoured. Cells are known to make a continuous contact with positively charged substrata, whereas in general, they present only discontinuous focal contacts with negatively charged substrata.
The measurement of the surface charge of a biopolymeric surface is hence an important in useful indicator of positive all-surface interaction. The measurement of the surface potential of polymer films was obtained with the Kelvin-probe technique. The Kelvin method was first postulated by the renowned Scottish scientist W. Thompson, later Lord Kelvin, in 1861. This method is based on the measurement of the potential difference between a fixed steel and vibrating plate, with and without a dielectric, positioning the two plates at a distance of a few millimetres. The difference between the two plates gives a measure of surface potential of the polymer (fig.7) [8].
The Kelvin Method is also an indirect technique for the measuring work function of a surface. The work function is the least amount of energy required to remove an electron from the surface of a conducting material, to a point just outside the metal, with zero kinetic energy. As the electron has to move through the surface region, it's energy is influenced by the optical, electric and mechanical characteristics of the region. Hence, the work function is an extremely sensitive indicator of surface condition and is affected by absorbed or evaporated layers, surface reconstruction, surface charging, oxide layer imperfections, surface and bulk contamination [9, 10, 11].

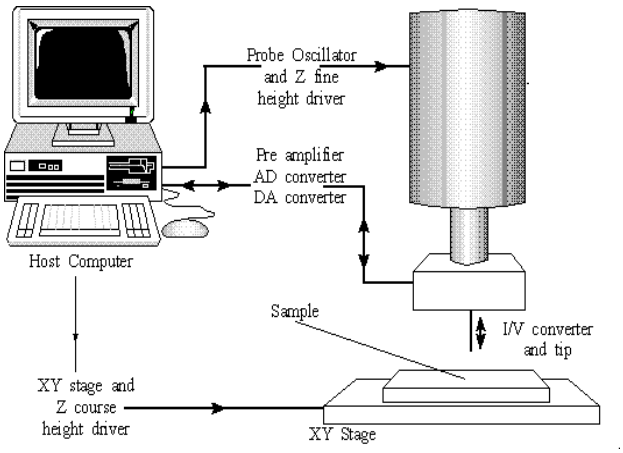

Fig. 7 A scheme of the Kelvin Probe device

By using a vibrating probe, a varying capacitance is produced. This is given by:

$$C = \frac{Q}{V} = \frac{\varepsilon_0 A}{d} \quad (3.13)$$

where C is the capacitance, Q is the Charge, V is the Potential, ε_0 is the permittivity of the dielectric (in an air probe the dielectric is air). A is the surface area of the capacitor and d is the separation between the plates. Therefore, as the separation d increases the capacitance C decreases. As the charge remains constant, the voltage V must increase

By the difference of potential it is possible to obtain, with an electric model, the surface charge density. The model is referred to a system constituted by two circular condensators, positioned in series, one that has air as dielectric and the second that has the polymeric film as dielectric. The thickness of film is supposed known and its surface flat. For this model the surface charge density is given by:

$$\sigma = \frac{2\varepsilon_0 \varepsilon V}{d(\varepsilon - 1) + R} \quad (3.14)$$

σ = Surface charge density
ε_0 = absolute dielectric constant
ε = Polymeric dielectric constant
V = potential difference between plate with and without polymer
d = thickness of polymeric film
R = radius of aluminium disc, utilised as substrate for the polymeric film

Cells, infact, adhere on both positively and negatively charged surfaces but the morphology of adhering cells may vary according to the sign of electrical charge.

Fluorimetry

Fluorimetry is a method of qualitative and quantitative chemical analysis of substances, based on the exam of analysis of the emitted light upon ultraviolet irradiation. This is possible because the characteristics of wavelength and intensity of the spectrum that are revealed with particular devices depends on the molecular structure of the substance. The intensity depends also on the quantity of substances present and this allows a quantitative analysis of concentration [12].

Light emission from atoms or molecules can be used to quantify the concentration of the phluorophore in a sample. The relationship between fluorescence intensity and analyte concentration is:

$$F = k * QE * P_o * (1\text{-}10^{[-*b*c]}) \quad (3.15)$$

where F is the measured fluorescence intensity, k is a geometric instrumental factor, QE is the quantum efficiency (photons emitted/photons absorbed), P_o is the radiant power of the excitation source, is the wavelength-dependent molar absorptivity coefficient, b is the path length, and c is the analyte concentration (b, and c are the same as used in the Beer-Lambert law).

The Beer-Lambert law (also called the Beer-Lambert-Bouguer law or simply Beer's law) is the linear relationship between absorbance and concentration of an absorber of electromagnetic radiation. The general Beer-Lambert law is usually written as:

$$A = a_\lambda \times b \times c$$

where A is the measured absorbance, a is a wavelength-dependent absorptivity coefficient, b is the path length, and c is the analyte concentration. When working in concentration units of molarity, the Beer-Lambert law is written as:

$$A = \varepsilon_\lambda \times b \times c$$

where is the wavelength-dependent molar absorptivity coefficient with units of $M^{-1}cm^{-1}$. The subscript λ is often dropped with the understanding that a value for is for a specific wavelength. If multiple species that absorb light at a given wavelength are present in a sample, the total absorbance at that wavelength is the sum due to all absorbers:

$$A = (\varepsilon_1 \times b \times c_1) + (\varepsilon_2 \times b \times c_2) + \ldots$$

Expanding equation (4.4) in series and dropping higher terms gives:

$$F = k * QE * P_o * (2.303 * * b * c) \quad (3.16)$$

This relationship is valid at low concentrations ($<10^{-5}$ M) and shows that fluorescence intensity is linearly proportional to analyte concentration.

Determining unknown concentrations from the amount of fluorescence that a sample emits requires calibration of a fluorimeter with a standard (to determine K and QE) or by using a working curve.

Many of the limitations of the Beer-Lambert law also affect quantitative fluorimetry. Fluorescence measurements are also susceptible to inner-filter effects. These effects include excessive absorption of the excitation radiation (pre-filter effect) and self-absorption of atomic resonance fluorescence (post-filter effect).

A spectrofluorimeter is the instrument used to measure fluorescence emitted by a substance. The reading of fluorescent light emitted by the molecules under examination, after their excitation with UV light, is detected using a reticular monocromator. The spectrophotometer is composed of a light source that traverses a monochromatic prism and constitutes the first incident ray I°. This traverses a cuvette containing the sample and exits with intensity I. This ray is detected by photoelectric cells, the current obtained is read with a galvanometer The measurement is made at 90° with respect to the UV source, in this manner the portion of incident radiation that is not absorbed by the samples is not detected. So, only the ultraviolet light absorbed by molecules and emitted as fluorescent is measured. Using fluorescent ligands, as albumin marked with fluorescein, it is possible show the absorption of adhesion protein on different type of samples. The scheme of the device used is shown in figure 8.

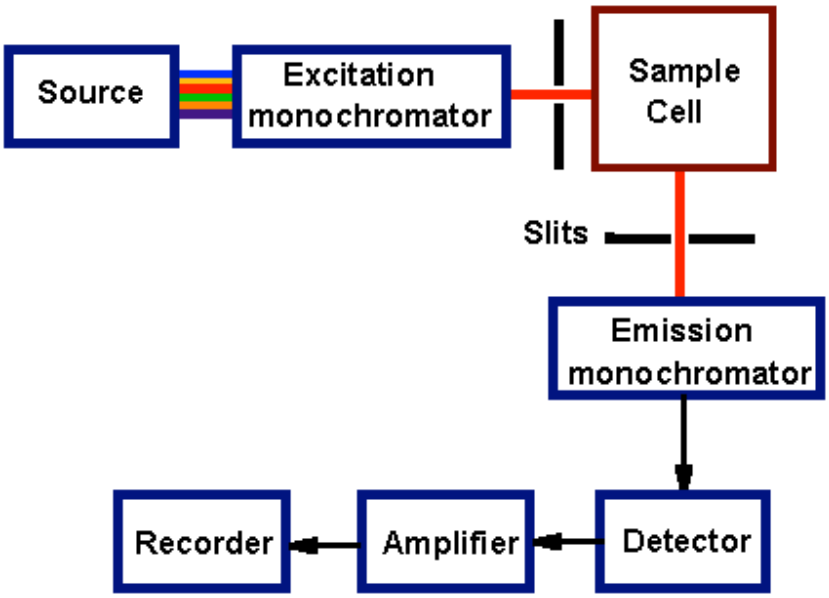

Fig.8 Scheme of a spectrophotometer

Scanning Electron Microscopy (SEM)

Scanning electronic microscopy allows the use of a wide range of magnifications, between 15 until 500000, and has a high depth of field, in other terms the difference between maximum and minimum focusing positions, which enables surfaces with high topographic variations to be well focused. In SEM the different points of a sample are explored with a high power thin electronic beam, produced by an electronic gun, and focused with a magnetic lens system. Appropriate devices allow either motions of beam, that allow exploring a little square area, on motions of the sample relative to the beam, that allow varying not only the area under examination but also the inclination of the sample relative to the beam [13, 14].

When a beam of electrons hits the surface of a material a part of these incident electrons, called primary electrons, preserve their energy and are reflected, (retrodiffusive electrons) (*e* in figure 9), while the other loose their energy by transferring it to the electrons of the solid, (*a, c* in figure 9). A fraction of electrons are then emitted with lower energy (*f, d* in figure 9).

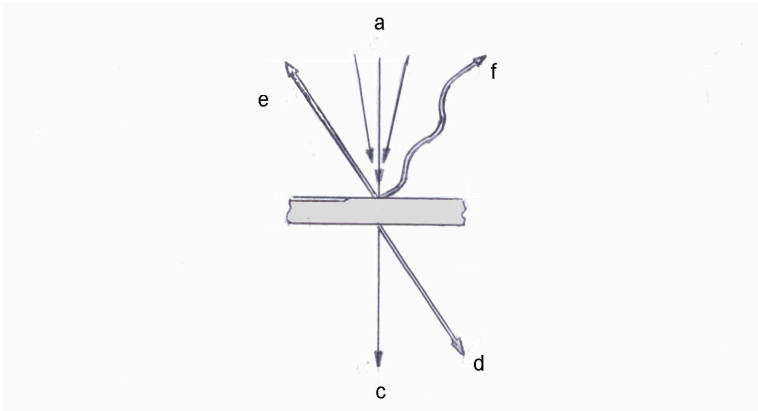

Fig. 9 Interaction of electronic beam against a solid surface

The incident electrons have high energy; they are able to ionise the interior energy levels of atoms of the material then go back to the fundamental state with photon emission. The X rays produced have energies that are characteristic of the atoms that emit them, and so they can be utilised to obtain information on the chemical composition of the sample. With an X-ray spectrum analyser, it is possibly have a spectrum that gives the relative peaks of the different elements. The intensity of characteristic line of one element is directly proportional to its concentration. Quantitative analyses are thus possible.
The samples examined can be the same as those used in optical microscopy, but they must be sufficiently conductive. To render them conductive sometimes a thin metallic layer is evaporated on the surface of these samples.
The main advantage of SEM is its high lateral and vertical resolution, enabling topographic information to be obtained (fig. 10-11).

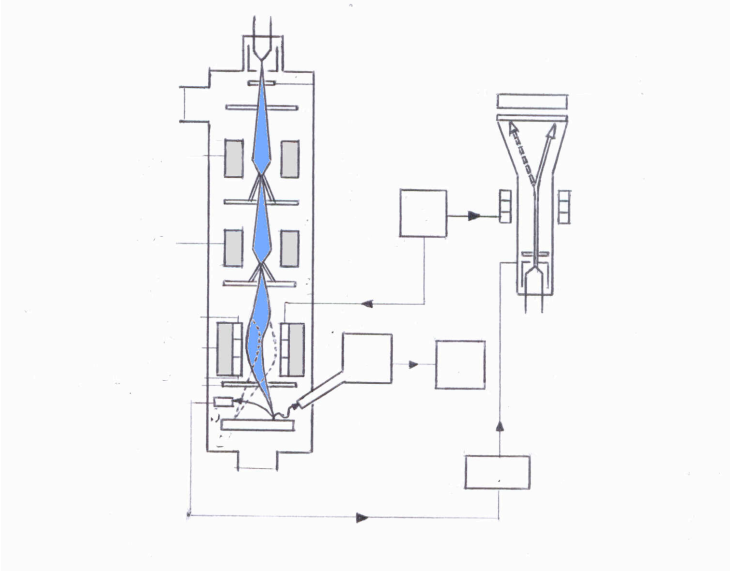

Fig.10 Internal scheme of a SEM.

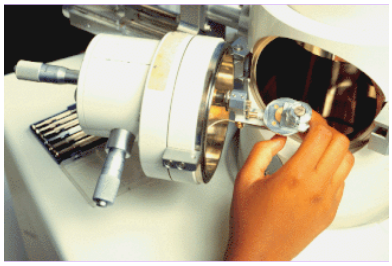

Fig.11 A commercial example of SEM with the analysis chamber on the right.

This instrument is present at faculty of Mechanical Engineering at university of Pisa.

Saybolt viscometer

To develop the model of microsyringe deposition it was necessary to measure the viscosity of the polymeric solutions used: a Saybolt viscometer, at Faculty of Chemistry of University of Pisa.
The flow behaviour of polymer melts is often a very important parameter in industrial processes and is particularly relevant to injection moulding. The viscosity of the melt is the single most important characteristic to be considered when designing polymer systems for ease of injection moulding [15]. In shear flow of a Newtonian liquid the shear stress is directly proportional to the shear strain rate and viscosity is independent of the shear rate, but several responses are possible for a polymer, as illustrated in figure 12:

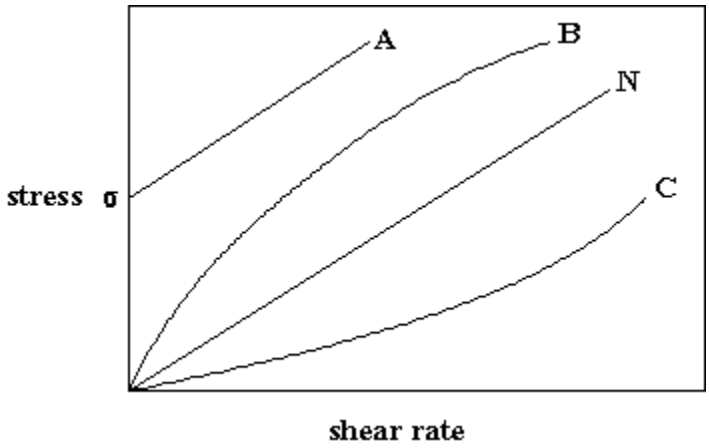

Fig. 12 Various types of viscosity behaviour in polymers

For two of the four types of viscosity behaviour illustrated stress is proportional to shear rate - these are the standard Newtonian (N) and Newtonian after a critical yield stress has been exceeded (A). The behaviour characterised by B and C is shear-rate thinning or pseudo plastic (B) and shear rate thickening or dilatent (C); several other types are possible. If the apparent viscosity is defined as the ratio of shear stress to strain rate or the slope of the plot, then it can be seen that for the case of pseudoplastics the apparent viscosity decreases as the shear rate increases whereas for dilatents the apparent viscosity increases - hence the terms shear thinning and shear thickening. In general polymer solutions or melts display shear-thinning behaviour. It is often possible to describe non-Newtonian flow by an empirical power law:

$$\sigma = K\left(\frac{dc}{dt}\right)^{n} \quad (3.17)$$

where K and n are constants. If n=1 then the expression reduces to Newton's Law for Newtonian fluids. For shear thinning fluids n is less than one and for shear thickening fluids n is greater than one. At the chemical level specific interactions such as hydrogen bonding will increase viscosity as they increase the energy barrier to flow. Sterically hindered molecules have a similar restriction, in general more flexible chains are associated with lower viscosity. A similar empirical power law to the one above has been useful in predicting viscosity as a function of concentration and molecular weight.

Above a critical molecular weight the zero shear viscosity (the steady state viscosity at zero shear rate) can be described by:

$$\eta = K' c^{\partial} \overline{M_w^{3.4}} \quad (3.18)$$

Known these law it is necessary have an apparatus to measure this viscosity, the most used apparatus is the Saybolt viscometer**.** It consists of a cylindrical container for the polymer solution under examination with a receiving flask under it to catch and measure polymer solution discharged from the container. At the bottom of the container is an orifice of specified dimensions through which the polymer flows. The container is jacketed with a water bath to facilitate maintenance of a constant temperature. Two thermometers check temperatures, one in the polymer solution and one in the water bath. To adjust the temperature, an external source of heat is applied to the bath. Flow of polymer solution into the receiver is timed with a stop watch or equivalent device. The time of flow is taken to be proportional to the viscosity of the fluid.
Viscosity is a linear function of temperature and it is possible express it as:

$$\mu = aT + b. \quad (3.19)$$

Considering the variation data of viscosity with the temperature, as present in literature, it was possible obtain that acetone viscosity law is:

$$\mu_{acetone} = 0.399 - 0.0016T \quad (3.20)$$

Our experiments were conducted at 22.5^0C where μ=0.363. The viscosity is also a linear function of the time:

$$\mu = \rho C_1 t \quad (3.21)$$

where C_1 is a constant depending on the measurement device and is independent of the solution. For acetone a value of $C_1 = \mu_{acetone}(22.5^0) = / \rho t = 1.761 * 10^{-2}$ was obtained.
Using 3.21, it was possible measure the viscosity of the polymeric solution, knowning its density and the times measured using the Saybolt viscometer.
In figures 13a and 13b the viscosity of PLLA and PCL solutions are plotted as a function of concentration.

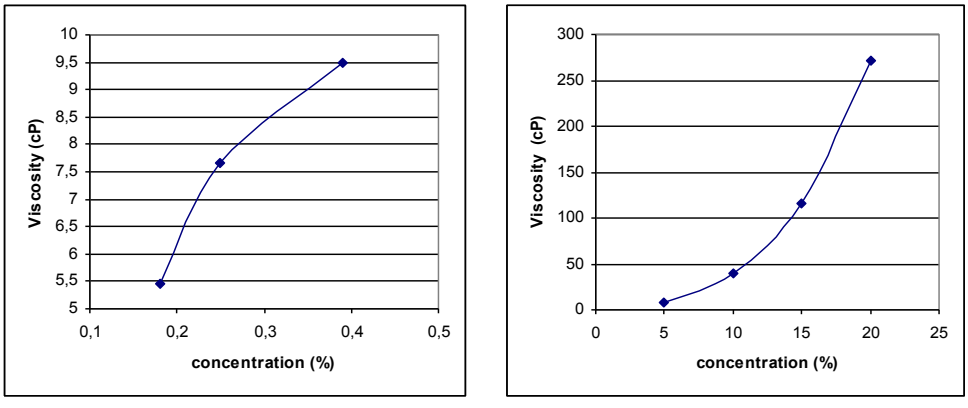

(a) (b)

Fig. 13 (a) Viscosity of PLLA as a function of concentration (b) Viscosity of PCL as a function of concentration.

Atomic Force Microscopy (AFM)

Binnig, Quate and Gerber invented the atomic force microscope (AFM) or scanning force microscope (SFM) in 1986. Like all other scanning probe microscopes, the AFM utilises a sharp probe moving over the surface of a sample in a raster scan. In the case of the AFM, the probe is a tip on the end of a cantilever, which bends in response to the force between the tip and the sample [16, 17].
The first AFM used a scanning tunnelling microscope at the end of the cantilever to detect the bending of the lever, but now most AFM employ an optical lever technique. The diagram (fig. 14) illustrates how this works; as the cantilever flexes, the light from the laser is reflected onto the split photo-diode. By measuring the difference signal (A-B), changes in the bending of the cantilever can be measured. Since the Cantilever obeys Hooke's Law for small displacements, the interaction force between the tip and the sample can be found. An extremely precise positioning device made from piezoelectric ceramics, most often in the form of a tube scanner performs the movement of the tip or sample. The scanner is capable of sub-angstrom resolution in x-, y- and z-directions. The z-axis is conventionally perpendicular to the sample.

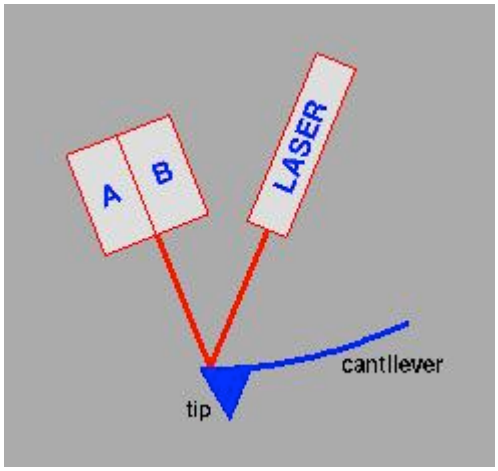

Fig.14 Operating principle of AFM

The AFM can be operated in two principal modes

- with feedback control
- without feedback control

If the electronic feedback is switched on, then the positioning piezo which is moving the sample (or tip) up and down can respond to any changes in force which are detected, and alter the tip-sample separation to restore the force to a pre-determined value. This mode of operation is known as *constant force*, and usually enables a fairly faithful topographical image to be obtained (hence the alternative name, *height mode*).
If the feedback electronics are switched off, then the microscope is said to be operating in *constant height* or *deflection* mode. This is particularly useful for imaging very flat samples at high resolution. Often it is best to have a small amount of feedback-loop gain, to avoid problems with thermal drift or the possibility of a rough sample damaging the tip and/or cantilever. Strictly, this should then be called *error signal* mode.
The error signal mode may also be displayed whilst feedback is switched on; this image will remove slow variations in topography but highlight the edges of features.
The way in which image contrast is obtained can be achieved in many ways. The three main classes of interaction are *contact mode*, *tapping mode* and *non-contact mode*.

Contact mode is the most common method of operation of the AFM. As the name suggests, the tip and sample remain in close contact as the scanning proceeds. By "contact" we mean in the repulsive regime of the inter-molecular force curve (see figure 15).

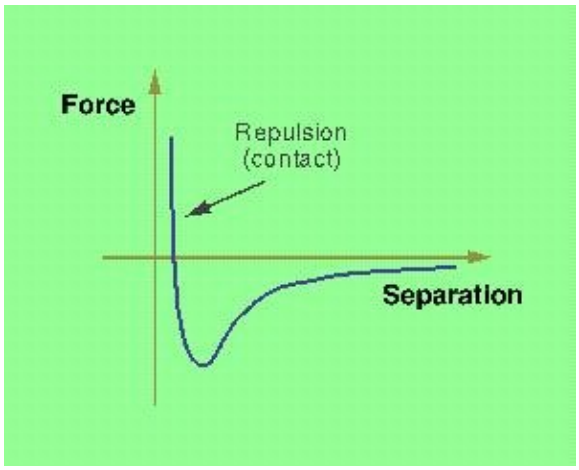

Fig.15 Interaction force in the Contact mode

The repulsive region of the curve lies above the x-axis. One of the drawbacks of remaining in contact with the sample is that there exist large lateral forces on the sample as the drip is "dragged" over the specimen.

Tapping mode is the next most common mode used in AFM. When operated in air or other gases, the cantilever is oscillated at its resonant frequency (often hundreds of kilohertz) and positioned above the surface so that it only taps the surface for a very small fraction of its oscillation period. This is still contact with the sample in the sense defined earlier, but the very short time over which this contact occurs means that lateral forces are dramatically reduced as the tip scans over the surface. When imaging poorly immobilised or soft samples, tapping mode may be a far better choice than contact mode for imaging (fig.16).

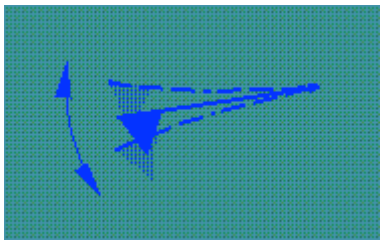

Fig.16 Operating principle of tapping mode

Other (more interesting) methods of obtaining image contrast are also possible with tapping mode. In constant force mode, the feedback loop adjusts so that the amplitude of the cantilever oscillation remains (nearly) constant. An image can be formed from this amplitude signal, as there will be small variations in this oscillation amplitude due to the control electronics not responding instantaneously to changes on the specimen surface.
More recently, there has been much interest in **phase** imaging. This works by measuring the phase difference between the oscillations of the cantilever driving piezo and the

detected oscillations. It is thought that image contrast is derived from image properties such as stiffness and viscoelasticiy.
Non-contact operation is another method, which may be employed when imaging by AFM. The cantilever must be oscillated above the surface of the sample at such a distance that we are no longer in the repulsive regime of the inter-molecular force curve. This is a very difficult mode to operate in ambient conditions with the AFM. The thin layer of water contamination, which exists on the surface on the sample, will invariably form a small capillary bridge between the tip and the sample and cause the tip to "jump-to-contact". Even under liquids and in vacuum, jump-to-contact is extremely likely, and imaging is most probably occurring using tapping mode.
One of the most important factors influencing the resolution, which may be achieved with an AFM, is the sharpness of the scanning tip. The first tips used by the inventors of the AFM were made by gluing diamond onto pieces of aluminium foil. Commercially fabricated probes are now universally used. The best tips may have a radius of curvature of only around 5nm. The need for sharp tips is normally explained in terms of *tip convolution*. This term is often used (slightly incorrectly) to group together any influence, which the tip has on the image. The main influences are

- broadening
- compression
- interaction forces
- aspect ratio

Tip broadening arises when the radius of curvature of the tip is comparable with, or greater than, the size of the feature trying to be imaged. The diagram illustrates this problem (fig. 17); as the tip scans over the specimen, the sides of the tip make contact before the apex, and the microscope begins to respond to the feature. This is what we may call tip convolution.

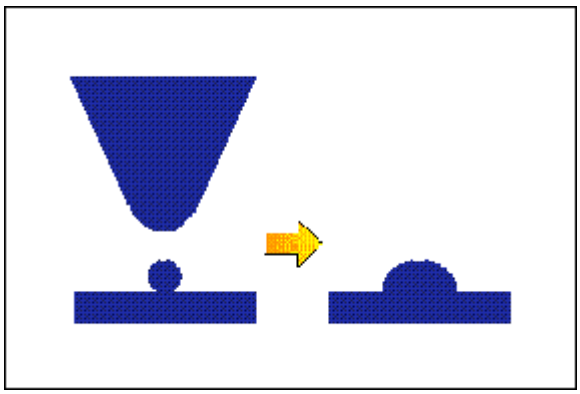

Fig. 17 Problem if tip broadening

Compression occurs when the tip is over the feature trying to be imaged. It is difficult to determine in many cases how important this affect is, but studies on some soft biological polymers (such as DNA) have shown the apparent DNA width to be a function of imaging force.
This device was used to characterise polymeric patterns. Measurements were performed at the CNR Biophysics Institute in PISA.

8 Fluorescence microscopy

Fluorescence microscopy is used to detect structures, molecules or proteins within the cell [14]. Fluorescent molecules absorb light at one wavelength and emit light at another, longer wavelength. When fluorescent molecules absorb a specific absorption wavelength for an electron in a given orbital, the electron rises to a higher energy level (the excited) state. Electrons in this state are unstable and will return to the ground state, releasing energy in the form of light and heat. This emission of energy is fluorescence. Because some energy is lost as heat, the emitted light contains less energy and therefore is a longer wavelength than the absorbed (or excitation) light. In fluorescence microscopy, a cell is stained with a dye and the dye is illuminated with filtered light at the absorbing wavelength; the light emitted from the dye is viewed through a filter that allows only the emitted wavelength to be seen. The dye glows brightly against a dark background because only the emitted wavelength is allowed to reach the eyepieces or camera port of the microscope. Most microscopes are designed using epi-illumination. In epi-illumination excitation, light goes through the objective lens and illuminates the object. Light emitted from the specimen is collected by the same objective lens (figs. 12-13).
Sometimes the fluorescent molecule itself is a direct stain or probe for specific structures. In other situations the fluorescent dye is bound to another non-fluorescent probe that recognises specific structures. For example, the fluorescence molecule, rhodamine, may be conjugated to phalloidin, which binds the filamentous actin. One important method to identify specific proteins is to couple fluorescent dyes to antibodies that bind very specifically to macromolecules in the cell.
Among the common fluorescence dyes are fluorescein, which emits green light when exited with blue light and rhodamine, which emits a deep red fluorescence when excited by green-yellow light. The fluorescence microscopes are equipped with three fluorescent filter cubes, each containing specific barrier filters and a beam-splitting mirror. The filter cubes provide blue light excitation (fluorescein), green light excitation (rhodamine), and UV excitation (for UV absorbing dyes).

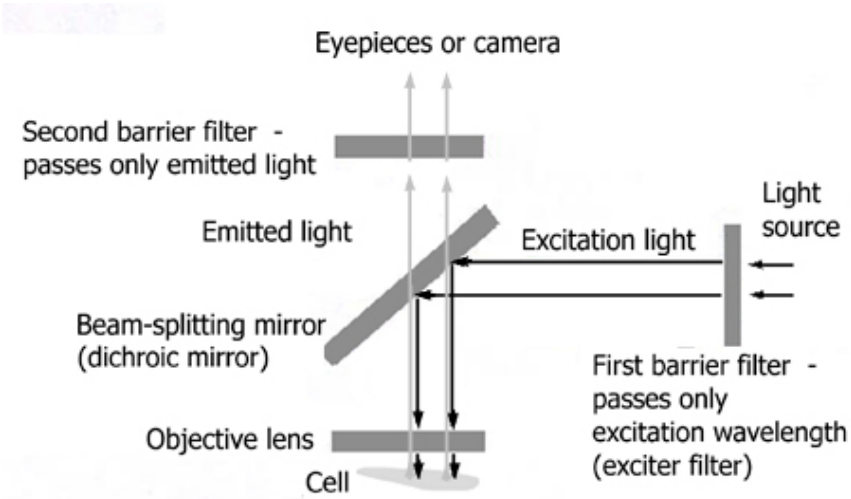

Fig.12 The optical system of an upright epi-fluorescence microscope

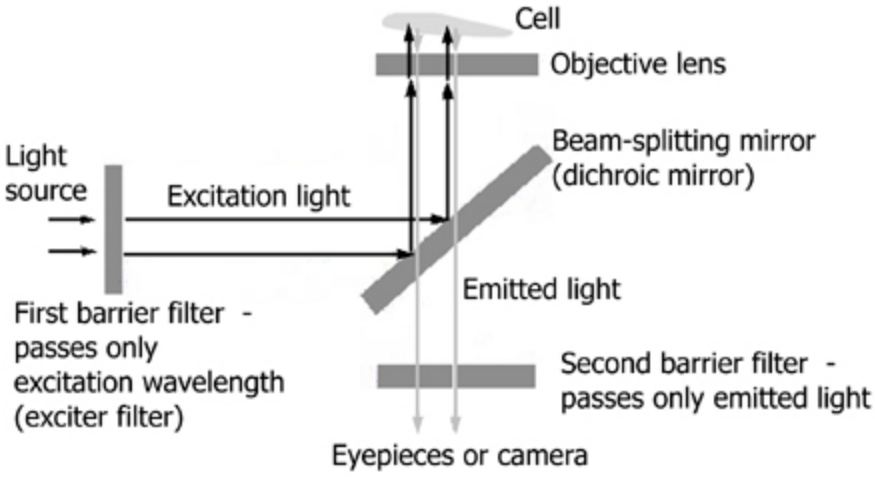

Fig.13 The optical system of an inverted epi-fluorescence microscope

Confocal Microscopy

The popularity of confocal microscopy arises from its ability to produce blur-free, crisp images of thick specimens at various depths. Confocal imaging rejects the out-of-focus information by placing a pinhole in front of the detector, so that only the region of the specimen that is in focus is detected. Confocal imaging can only be performed with point wise illumination and detection, which is an important advantage of using laser-scanning microscopy.

Light from a laser passes through a small pinhole (figure 14) and expands to fill the entrance pupil of a microscope objective lens. The objective lens focuses the light to a small spot on the specimen, at the focal plane of the objective lens. Light reflected back from the illuminated spot on the specimen is collected by the objective and is partially reflected by a beam splitter to be directed at a pinhole placed in front of the detector. This confocal pinhole is what gives the system its confocal property, by rejecting light that did not originate from the focal plane of the microscope objective. Light rays from below the focal plane come to a focus before reaching the detector pinhole, and then they expand out so that most of the rays are physically blocked from reaching the detector by the detector pinhole. In the same way, light reflected from above the focal plane focuses behind the detector pinhole, so that most of that light also hits the edges of the pinhole and is not detected. However, all the light from the focal plane is focused at the detector pinhole and so is detected at the detector. This ability to reject light from above or below the focal plane enables the confocal microscope to perform depth discrimination and optical tomography. A true 3D image can be processed by taking a series of confocal images at successive planes into the specimen and assembling them in computer memory.

Confocal microscopy was used to test and measure the cell adhered on three-dimensional microstructures [19, 20].

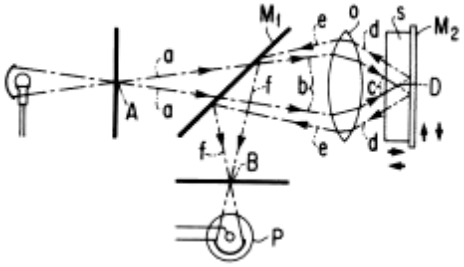

Fig. 14 Pattern of light in a confocal microscopy

Bibliography

[1] C. Allain, D. Auserre, F. Rundelez, *A new method for contact angle measurements of sessile drops, Journal of Colloid and Interface,* Science September 1985, vol. 107, n.1, pp. 5-13.

[2] *Contact Angle Meausurements with sessile drops and bubbles*, Journal of Colloid and Interface Science August 1991, vol.145, n.1, pp. 279-282.

[3] J.D. Andrade, *Surface and Interfacial aspects of biomedical polymers*, Plenum Press. New York and London 1985, vol.1, pp. 113-125.

[4] A.W. Adamson, *Physical Chemistry of surface*, 5th Edition, John Wiley & Sons Inc. New York 1990, pp.389-402.

[5] J.D. Andrade, *Surface and Interfacial aspects of biomedical polymers*, Plenum Press. New York and London 1985, vol.1, pp. 265-273.

[6] M. McCrackin, E. Passaglia, R.R. Stromberg, H.L. Stainberg, *Measurement of the thickness and refractive index of very thin films and the optical properties of surfaces by Ellipsometry*, Journal of Research August 1963, vol. 67/a, n.4, pp. 363-377.

[7] R.M.A. Azzam, N.M. Bashara, *Ellipsometry and polarized light*, North-Holland Physics publishing Amsterdam 1987.

[8] I.D. Baikie, S. Mackenzie, P.J.Z. Estrup and J.A. Meyer*, Noise and the Kelvin Method*,Rev. Sci. Instrum., **62**1326 (1991).

[9] G. Bruggink and I.D. Baikie*, Preliminary studies on stress in metals, employing the Kelvin Method*, Proc. Residential Stress Conf., Univ. of Twente (1991).

[10] I.D. Baikie and G. Bruggink*, Characterisation of Surface Preparation Methods using a Scanning Kelvin Probe*, Mat. Res. Soc. Proc., 315, 311 (1993).

[11] I.D. Baikie and G. Bruggink, Mat. Res. Soc. Proc., *Thin Film Characterisation*, 309, 35 (1993).

[12] Ichinose N, Schwedt G, Adachi K, Schnepel FM, *Fluorometric Analysis in Biomedical Chemistry Chemical Analysis:A Series of Monographs on Analytical Chemistry and Its Applications*, Hardcover, 1991, publisher: John Wiley & Sons.

[13]Heywood, V. H., editor, 1971. *Scanning Electron Microscopy: Systematic and Evolutionary Applications*. Systematics Association Special Volume 4, Academic Press, London and New York.

[14] Wolfe SL, *Introduzione alla biologia cellulare e molecolare*, EdiSES 1996.

[15] Jokuty P,Whiticar S, Wang Z, Fingas M, Lambert P, Fieldhouse B, Mullin B, *A crude catalogue of crude oil and oil product properties, Biomaterials*, vol.11, 1976, pp.35-43.

[16] Morris VJ, Kirby RB, Gunning AP, *Atomic Force Microscopy for biologists*, December 1999,Wiley & Sons

[17] Mukhopadhyay, R. and J. H. Hoh**,** *AFM force measurements on microtubule-associated proteins: the projection domain exerts a long-range repulsive force***.** (2001). FEBS Lett. 505 : (3) 374-378.

[18]Matsumoto, B., ed. (1993). *Cell biological applications of confocal microscopy*, Academic Press. San Diego, California.

[19] Pawley, J. B., ed. (1990). *Handbook of Biological Confocal Microscopy*.,Plenum, New York.

[20] Diaspro A, Beltrame F, Fato M, Ramoino I, *Characterising Biostructures and cellular events in 2D/3D,* IEEE Engineering in Medicine and Biology, Jan/Feb 1996, pp. 92-100.